

Effect of general loss-cone distribution function on EIC waves in multi- component plasma-particle aspect approach

B D Raikwar*, P Varma & M S Tiwari

Department of Physics, Dr H S Gour Vishwavidyalaya, Sagar 470 003, India

Received 30 December 2016; revised received 09 March 2017; accepted 13 April 2017

Electrostatic ion-cyclotron waves are investigated in multi-ion plasma (H^+ , He^+ and O^+) using particle aspect analysis. Variations with perpendicular wave number of wave frequency, resonant energy and growth rate with general loss-cone distribution function are studied. The whole plasma is considered to consist of resonant and non-resonant particles. The resonant particles participate in energy exchange while the non-resonant particles support the oscillatory motion of the wave. The wave is assumed to propagate obliquely to the static magnetic field. It is found that the frequency for the lighter ions increases then decreases by increasing the perpendicular wave number while the frequency for the heavier ions is constant. Perpendicular wave number decreases the growth rate of the wave and also decreases perpendicular resonant energy and increases parallel resonant energy. The effect of general loss-cone distribution is also discussed with multi-component plasma which increases the wave frequency, growth rate and parallel resonant energy while decreases the perpendicular resonant energy. The study may explain the EIC waves observed in auroral acceleration region. The results are interpreted for the space plasma parameters appropriate to the auroral acceleration region around the earth's magnetosphere.

Keywords: Electrostatic ion-cyclotron waves, Particle aspect approach, Resonant particles, Non-resonant particles, Auroral acceleration region, Loss-cone distribution Function

1 Introduction

The excitation of ion-cyclotron waves has received considerable attention because they provide an efficient mechanism for energization of cold ionospheric ions perpendicular to the Earth's magnetic field¹. These ions are driven upward along the Earth's diverging magnetic field lines by the mirror force, converting some of their perpendicular energy into parallel energy forming ion beams and conic distributions. These transversely accelerated ions of ionospheric origin ultimately make their way deep into the magnetosphere, accounting for a significant population of hot magnetospheric ions². Electrostatic ion-cyclotron (EIC) waves have also been discussed as a possible mechanism for the formation of V-shaped electric potential structures in the auroral ionosphere, connected directly to the earthward acceleration of auroral electrons, have been observed simultaneously with EIC waves. The investigation of charged particle trajectories, in the presence of wave paves, the way to study the excitation of waves, their dispersion relations, current driven by the waves and the transfer of energy to the particles and hence heating and acceleration of the charged particles by the wave, in the

same sequence of analysis, referred to as the particle aspect analysis, which will be adopted in the present investigation.

Ono *et al.*³ studied the parametric excitation of EIC waves in the He^+-Ne^+ plasma. Abraham *et al.*⁴ found that the wave can be driven unstable by the hydrogen ion drift velocity alone, at small perpendicular wave number as well as electron drift velocity at large perpendicular wave number. Also, the growth rate is dependent on the densities and temperature anisotropies of the various constituent ions. Zhao *et al.*⁵ found that proportion of high and low energy outflow O^+ increased during magnetic storms. They also suggested that the O^+ outflow intensity increased from 2000 to 4200 km and had a positive correlation with the solar activities. Simic *et al.*⁶ have investigated the critical electron drift velocity in the presence of positively or negatively charged resonant ions in multi-component plasma they shown that the critical drift decreases' as the state of plasma approaches the isothermic state. Kurian *et al.*⁷ found that the frequencies and growth/damping rates are dependent on the densities and temperatures of all species of ions (H^+ , O^+ , O^-). They also studied that ion cyclotron waves are driven by electron drift parallel to the electric field; the temperature anisotropy of oxygen

*Corresponding author (E-mail: bhagwandr.90@gmail.com)

ions only slightly enhance the growth rates for small values of temperature anisotropies. Rosenberg *et al.*⁸ found that as the concentration of heavy negative ions increases, the wave frequencies increase, the unstable spectrum in general shifts to longer perpendicular wavelengths, and the growth of higher harmonic EIC waves tends to increase within certain parameter ranges. Ahirwar *et al.*⁹ have studied electromagnetic ion-cyclotron waves with multi-ion plasma (H^+ , He^+ , O^+) in auroral acceleration region of the earth magneto-plasma their conclusions may be useful to explain heating of He^+ , O^+ ions by particle aspect approach along with dynamics of EIC instability. It is found that the effect of plasma densities enhances the steepness of loss-cone distribution function.

The ground-satellite observations of structured dayside Pcl emissions related to magnetospheric compressions arise from enhanced densities in the solar wind¹⁰ type mechanism in the top side auroral ionosphere could be easily explained for the enhanced He^+ energization. The He^+ ions are accelerated with H^+ and O^+ and the consistent association between preferential acceleration and EIC waves may suggested by the cyclotron resonant acceleration mechanism. Ion heating and acceleration perpendicular to the magnetic field is a common feature in the auroral region. The observational evidence of simultaneous observations of ion cyclotron modes and perpendicular heating of ions are studied by Hamrin *et al.*¹¹, Summers *et al.*¹², Albert *et al.*¹³ and Engebreston *et al.*¹⁴. Kim Su-Hyun *et al.*¹⁵ shown that waves with frequencies near the ion gyro frequencies and multiple harmonics launched from an antenna are observed to grow in amplitude in the region of ion flow shear. They discussed implication of these results for plasma wave excitation in earth's auroral region. Strelstov¹⁶ presented the results from numerical study of the effect of multiple ion species on the development of small-scale, intense electromagnetic waves and density structures that are frequently observed in the auroral ionosphere in the vicinity of discrete auroral arcs. The simulations reveal that these waves can be generated by the ionospheric feedback instability in the downward current channels adjacent to the upward currents, causing aurora, when heavy ionospheric ions in particular (O_2^+) provide the "matching impedance" condition between the ionosphere and the magnetosphere. Pandey *et al.*¹⁷ studied the oblique electromagnetic electron cyclotron waves for Kappa distribution with A. C. field in planetary magnetospheres.

The problem of EIC wave excitation in such a case was first studied by Kindel and Kennel¹⁸ using the kinetic theory developed earlier by Drummond and Rosenbluth¹⁹. There have been a few experiments on EIC waves in multi-ion species plasmas. In previous work various authors Mishra and Tiwari *et al.*²⁰ studied the EIC waves in single ion plasma, thus it has become necessary to understand the excitation of EIC waves in multispecies plasmas. The importance of ion cyclotron waves in auroral physics lies in their ability to heat and accelerate ions, and perhaps to provide anomalous resistivity, allowing the creation of a parallel potential drop. Since such processes have global implications for the magnetosphere, these waves have been the subject of numerous publications²¹⁻²⁵ and shown the existence of electromagnetic waves. Chaston *et al.*²⁶ have shown that these waves can have a Poynting flux directed upward out of the auroral oval, suggesting that the waves observed at higher altitudes may have their source at the base of the auroral potential structure where they are electromagnetic.

The motion of an electrically charged particle in a magnetic field can be treated as the superposition of a relatively fast circular motion around a point called the guiding center and a relatively slow drift of this point. The drift speeds may differ for various species depending on their charge states, masses, or temperatures, possibly resulting in electric currents. These differences in various parameters of different species will be used to study the effect of multi-ions, i.e., H^+ , He^+ and O^+ ions present in earth's magnetosphere. Different ion species exhibits different dynamics, depending on their masses and initial distributions. Trapped charged particles drift slowly around Earth, to gyrate around their guiding field lines and bouncing back and forth between mirror points, switching guiding field lines but staying at approximately the same distance.

The EIC turbulence plays an important role in the loss-cone current potential relationship. It has been suggested that the loss-cone effects can enhance the anomalous resistivity for a given turbulence level. Since the steep loss-cone distribution in the presence of EIC waves and the multi-ions enhances the growth rate, the anomalous resistivity and transport resulting from this instability are likely to play a crucial role in the auroral acceleration region. The converging magnetic field lines in the higher latitude auroral ionosphere may be considered suitable for the use of the generalized loss-cone distribution function. Pitch angle of a charged

particle increases as it moves into a region of stronger magnetic field and decreases as it moves into a region of weaker field. In simple magnetic mirror geometry, the magnetic field reaches a minimum value at the centre of the geometry because the spacing between fields lines greater diverging in nature. For the ends and magnetic field is at maximum value due to converging nature of magnetic field lines. The particles within this geometry can follow a range of trajectories to be confined; this result is known as magnetic mirroring. The particle briefly gyrates perpendicular to its guiding field line, and then retreats back to the weaker field, the spiral unwinding again in the process.

Magnetic mirror is a type of magnetic confinement device, used in physics experiments to trap high temperature plasma using magnetic fields. In a magnetic mirror, a specially shaped electromagnet creates a configuration of magnetic field lines, which reflects charged particles from a high-density magnetic field region to a low-density magnetic field region as discussed above. This mirror effect will only occur for particles within a limited range of velocities and angles of approach. Plasma in a mirror like device and in the auroral region with curved and converging magnetic field lines considerably depart from Maxwellian distribution and have steep loss-cone distribution function. It has been widely used by many researchers on the study of electrostatic waves, electrostatic ion-cyclotron waves^{27,28}, and electromagnetic waves, drift waves²⁹, electromagnetic ion-cyclotron waves^{8,9}.

The auroral acceleration region follow the geometry of mirror like devices, the use of general loss-cone distribution may be more appropriate to describe EIC waves in the auroral region. The general loss-cone distribution has been adopted by various authors^{30,31} in past. Here index J represents the effectiveness of perpendicular velocity and specify the effectiveness of mirror geometry. Increasing the value of J , which appears as the power on V_{\perp} reflects that the particles are having much more perpendicular velocity as compared to the parallel velocity. $J=1$ and $J=2$ represents steeper distributions.

In this paper, we have studied a systematic and detailed investigation of EIC waves in multi-component plasma with general loss-cone distribution function for magnetosphere like plasma parameters, with the purpose of attaining a more complete understanding of their relative importance. The advantage of present approach is to its suitability for dealing with auroral electrodynamics involving the

heating, acceleration and energy exchange by wave particle resonant interaction.

2 Basic Trajectory

An EIC wave is assumed to start at $t=0$ when the resonant particles are not disturbed. The trajectories of particles are then evaluated within the framework of linear theory. The wave is assumed to have the form:

$$K_{\parallel} E, k = (k_{\perp}, 0, k_{\parallel}), E = (E_x, 0, E_z)$$

with

$$E_x(r, t) = E_1 \cos(k_{\perp} x + k_{\parallel} z - \omega t),$$

$$E_z(r, t) = \kappa E_1 \cos(k_{\perp} x + k_{\parallel} z - \omega t)$$

and

$$\kappa = \left(\frac{k_{\parallel}}{k_{\perp}} \right) < 1$$

The amplitude E_1 is slowly varying function of t , i.e.,

$$\frac{1}{E_1} \left(\frac{dE_1}{dt} \right) \ll \omega$$

The EIC instability in the system of hot electrons and hot ions is considered under the condition:

$$V_{T\parallel\alpha} < \left| \frac{\omega - \lambda \Omega_{\alpha}}{k_{\parallel}} \right| \ll V_{T\parallel e}$$

$$\text{and } k_{\perp}^2 \rho_e^2 \ll k_{\perp}^2 \rho_{\alpha}^2 \sim 1$$

Where $V_{T\parallel\alpha,e}$ is the thermal velocity of the ions and electrons, respectively along the magnetic field, Ω_{α} is the ion-cyclotron frequency. $\lambda = 1, 2, \dots$ represent the harmonics of the wave, $\rho_{i,e}$ is the mean gyro-radii of the ions and electrons, respectively, k_{\parallel} and k_{\perp} are the components of the wave vector along and across the magnetic field, respectively and ω represents the wave frequency.

2.1 Trajectories and velocities of the particles

The trajectories of particles are evaluated within the framework of linear theory. The equation of motion of a particle is given by:

$$m \left(\frac{dv}{dt} \right) = q \left[E + \left(\frac{1}{c} \right) v \times B_0 \right] \quad \dots (1)$$

If E is considered to be a small perturbation, i.e., $E = E_1$, velocity v can be expressed in terms of unperturbed velocity V and perturbed velocity u .

Then the trajectory of the free gyration is obtained as;

$$\begin{aligned} X(t) &= \frac{V_{\perp}}{\Omega_{\alpha}} [\sin(\theta - \Omega_{\alpha}t) - \sin \theta] + X_0, \\ Y(t) &= \frac{V_{\perp}}{\Omega_{\alpha}} [\cos(\theta - \Omega_{\alpha}t) - \cos \theta] + Y_0, \quad \dots (2) \\ Z(t) &= V_{\parallel}t + Z_0 \end{aligned}$$

The perturbed velocity u is determined by:

$$\begin{aligned} \frac{du_{\perp}}{dt} + i\Omega_{\alpha}u_{\perp} &= \frac{qE_1}{m} \sum_{-\infty}^{+\infty} j_l(\mu) \cos(A_{\lambda}t + \psi_{\lambda}^0) \\ \frac{du_{\parallel}}{dt} &= \frac{qE_1}{m} \sum_{-\infty}^{+\infty} j_l(\mu) \cos(A_{\lambda}t + \psi_{\lambda}^0) \quad \dots (3) \end{aligned}$$

Where $u_{\perp} = u_x + iu_y$ represents the perturbed velocity in transverse direction and u_{\parallel} represents the velocity in parallel direction. The resonance criteria are given by:

$$\begin{aligned} A_{\lambda}(V_{\parallel} = V_r) &= k_{\parallel}V_{\parallel} - \omega + \lambda\Omega_{\alpha} \\ &= 0; \lambda = \pm 1, \pm 2, \pm 3, \dots \end{aligned}$$

Where, V_r is the resonance velocity of the particles

The oscillatory solution of $u(t)$ is given by:

$$\begin{aligned} u_x(r, t) &= \frac{qE_1}{m} \sum_{-\infty}^{+\infty} J_n(\mu) \sum_{-\infty}^{+\infty} J_{\lambda}(\mu) \times \\ &\left[\begin{aligned} &\frac{A_{\lambda}}{A_{\lambda}^2 - \Omega_{\alpha}^2} \sin \chi_{nl} - \\ &\frac{\delta}{2A_{\lambda+1}} \sin(\chi_{nl} - A_{\lambda+1}t) - \\ &\frac{\delta}{2A_{\lambda-1}} \sin(\chi_{nl} - A_{\lambda-1}t) \end{aligned} \right] \\ u_y(r, t) &= \frac{qE_1}{m} \sum_{-\infty}^{+\infty} J_n(\mu) \sum_{-\infty}^{+\infty} J_{\lambda}(\mu) \times \\ &\left[\begin{aligned} &\frac{A_{\lambda}}{A_{\lambda}^2 - \Omega_{\alpha}^2} \cos \chi_{nl} - \frac{\delta}{2A_{\lambda+1}} \cos(\chi_{nl} - \\ &A_{\lambda+1}t) - \frac{\delta}{2A_{\lambda-1}} \cos(\chi_{nl} - A_{\lambda-1}t) \end{aligned} \right] \\ u_z(r, t) &= \frac{q\kappa E_1}{m} \sum_{-\infty}^{+\infty} J_n(\mu) \sum_{-\infty}^{+\infty} J_{\lambda}(\mu) \frac{1}{A_{\lambda}} \\ &[\sin \chi_{nl} - \delta \sin(\chi_{nl} - A_{\lambda}t)] \quad \dots (4) \end{aligned}$$

where, $\chi_{nl} = k.r - \omega t + (n - \lambda)(\Omega_{\alpha}t - \theta)$

$\delta = 0$ for non-resonant particles and $\delta = 1$ for resonant particles

2.2 Density perturbation

To determine the dispersion relation and the growth rate, we consider bi-Maxwellian plasma with density perturbation as

$$N(v) = N_0 f_{\perp}(v_{\perp}) f_{\parallel}(v_{\parallel}) \quad \dots (5)$$

$$f_{\perp}(v_{\perp}) = \left[\frac{v_{\perp}^{2J}}{\pi v_{T_{\perp}}^{2(J+1)} J!} \right] \exp\left(\frac{-v_{\perp}^2}{v_{T_{\perp}}^2} \right) \quad \dots (6)$$

$$f_{\parallel}(v_{\parallel}) = \left(\frac{1}{\sqrt{\pi} v_{T_{\parallel}}} \right) \exp\left(\frac{-v_{\parallel}^2}{v_{T_{\parallel}}^2} \right) \quad \dots (7)$$

Where J is distribution index and measures the steepness of loss-cone feature. It characterizes the width of loss cone^{28,29}. In case $J = 0$, this represents a Maxwellian distribution, $J = \infty$, this reduces to Dirac delta function, $\delta(V_{\perp} - J^{1/2}V_{T_{\perp}})$ and peaked about $J^{1/2}V_{T_{\perp}}$ and has a half width of $\Delta V \sim J^{-1/2}V_{T_{\perp}}$ given by Mishra and Tiwari³².

$V_{T_{\parallel}}^2 = \frac{2T_{\parallel}}{m_{\alpha}}$, and $V_{T_{\perp}}^2 = (j+1)^{-1} \frac{2T_{\perp}}{m_{\alpha}}$ are the squares of parallel and perpendicular velocities of multi ions with respect to the external magnetic field.

The quasi-neutrality condition yields to the equation:

$$n_e = n_{H^+} + n_{O^+} + n_{He^+}$$

Thus we evaluate the density perturbation associated with the particle velocity as:

$$\begin{aligned} \frac{dn_1}{dt} &= -N_{H^+}(v_{H^+})(\nabla \cdot u)_{H^+} + \\ &(-N_{He^+}(v_{He^+})(\nabla \cdot u)_{He^+}) + (-N_{O^+}(v_{O^+})(\nabla \cdot u)_{O^+}) \quad \dots (8) \end{aligned}$$

Transforming the RHS of Eq. (8) as the function of t and we get the solution of equation

$$n_1(r, t) = \frac{qE_1 N(v_{\alpha})}{m_{\alpha}} \kappa^2 k_{\perp} \sum_{l, n=-\infty}^{+\infty} J_{\lambda}(\mu) J_n(\mu) \left[\frac{k_{\perp}}{A_{\lambda}^2 - \Omega_{\alpha}^2} + \frac{\kappa^2 k_{\perp}}{\Lambda_{\lambda}^2} \right] \sin \chi_{nl}$$

and

$$\begin{aligned}
n_1(r, t) &= \frac{qE_1 N(v_{H^+})}{m_\alpha} k^2 k_\perp \\
&\sum_{l, n=-\infty}^{+\infty} J_1(\mu) J_n(\mu) \frac{1}{\Lambda^2} \\
&\left\{ \sin \chi_{nl} - \sin(\chi_{nl} - \wedge_{IH} t) - \wedge_{IH^+} t \cos(\chi_{nl} - \wedge_{IH^+} t) \right\} \\
&+ \frac{qE_1 N(v_{He^+})}{m_{He^+}} k^2 k_\perp \\
&\sum_{l, n=-\infty}^{+\infty} J_1(\mu) J_n(\mu) \frac{1}{\Lambda^2_{IH^+}} \\
&\left\{ \sin \chi_{nl} - \sin(\chi_{nl} - \wedge_{IHe} t) - \wedge_{IHe^+} t \cos(\chi_{nl} - \wedge_{IHe^+} t) \right\} \\
&+ \frac{qE_1 N(v_{O^+})}{m_{O^+}} k^2 k_\perp \\
&\sum_{l, n=-\infty}^{+\infty} J_1(\mu) J_n(\mu) \frac{1}{\Lambda^2_{Io^+}} \\
&\left\{ \sin \chi_{nl} - \sin(\chi_{nl} - \wedge_{IHe} t) - \wedge_{Io^+} t \cos(\chi_{nl} - \wedge_{Io^+} t) \right\} \\
&\dots (9)
\end{aligned}$$

Where and $\alpha = H, He^+, O^+$

2.3 Dispersion relation

The Poisson equation is,

$$\nabla \cdot E = -\kappa_\perp (1 + \kappa^2) E_1 \sin(\kappa \cdot r - \omega t) = 4\pi e (n_i - n_e) \quad \dots (10)$$

Where $n_{i,e}$ is integrated perturbed density of the non-resonant particles of the respective species given by,

$$n_{\alpha,e} = \mp \int dv N(v) \frac{eE_1 k_\perp}{m_{\alpha,e}} \sum_{nl} \left\{ J_n(\mu) J_l(\mu) \times \left(\frac{1}{\Lambda^2_n - \Omega_\alpha^2} + \frac{\kappa^2}{\Lambda^2} \right) \sin \chi_{nl} \right\}_{i,e} \quad \dots (11)$$

Where $\mu = \frac{k_\perp V_\perp}{\Omega_{\alpha,e}}, \wedge_n = k_\parallel V_\parallel - \omega + n\Omega_{i,e}$ and

$$\chi_{nl} = k \cdot r - \omega t + (n - l)(\Omega_\alpha l - \theta)$$

Where, $\alpha = H, He^+, O^+$

Using expression for unperturbed density for the non-resonant ions²⁰ and Eq. (5) the integrated perturbed densities for the non-resonant particles is derived as,

$$\begin{aligned}
n_e &\cong \left(\frac{1}{k_\perp d^2 \Pi_e} \right) \frac{E_1}{4\pi e} \sin(k \cdot r - \omega t) \\
\text{and } n_i &\cong - \frac{k_\perp \kappa^2 \omega_{p\alpha}^2}{[\omega - \lambda \Omega_\alpha]^2} \langle J^2_\lambda \rangle \frac{E_1}{4\pi e} \sin(k \cdot r - \omega t) \\
\langle J^2_\lambda \rangle &= \int_0^\infty 2\pi V_\perp dV_\perp J^2_l(\mu) f_{\perp\alpha}(V_\perp)
\end{aligned}$$

Where, $\omega_{p\alpha}^2 = \frac{4\pi N_\alpha e^2}{m_\alpha}$ is plasma frequency for

the multi ions and N_α the multi ions plasma density. Then the dispersion relation is,

$$\begin{aligned}
1 + \left(\frac{1}{1 + \kappa} \right) \left(\frac{1}{k_\perp^2 d^2 \Pi_e} \right) - \left(\frac{\kappa^2}{1 + \kappa} \right) + \\
\left(\frac{\omega_{p\alpha}^2}{(\omega - \lambda \Omega_\alpha)^2} \right) \langle J^2_{\lambda-1} - J^2_{\lambda+1} \rangle \geq 0 \quad \dots (12)
\end{aligned}$$

For $\lambda=1$, $\langle (J^2_0 + J^2_2) \rangle = 1 - (j+1) \frac{k^2_\perp \rho^2_\alpha}{2}$;

$$\langle (J_0 + J_2)^2 \rangle = 1 - \frac{1}{2} (j+1) \frac{k^2_\perp \rho^2_\alpha}{2}$$

For $J=0$, this dispersion relation reduces to that given by Terashima³³.

2.4 Growth rate

The wave energy per unit wavelength can be defined as

$$\begin{aligned}
W_w &= \frac{\lambda E_1^2}{8\pi} + W_e + W_\alpha \text{ where,} \\
W_{\alpha,e} &= \int_0^\lambda ds \int dV \frac{m_{e,\alpha}}{2} \left\{ (N + n_1)(V + u)^2 - NV^2 \right\}_{\alpha,e}, \\
W_w &\approx \frac{\lambda E_1^2}{8\pi} + \frac{\lambda E_1^2}{16\pi} \frac{\omega_{p\alpha}^2}{\{\omega - \lambda \Omega_\alpha\}^2} \kappa^2 \frac{1}{2} \quad \dots (13)
\end{aligned}$$

$$\langle J_{\lambda-1}^2 + J_{\lambda+1}^2 \rangle + \frac{\lambda E_1^2}{16\pi} \left(\frac{1}{k^2_\perp d^2 \Pi_e} \right)$$

2.5 Rate of energy transfer

The changes in energy of the resonant particles are,

$$\begin{aligned}
W_r &= \sum_{i,e} (W_{r\perp} + W_{r\parallel}) \\
W_{r\perp} &= \int_0^\lambda ds \int_0^\infty V_\perp dV_\perp \int_0^{2\theta} \int_{v_r - \Delta r}^{v_r + \Delta r} d\theta \int dV_\parallel \frac{m_\alpha}{2} \left\{ (N + n_1)(V_\perp + u_\perp)^2 - NV_\perp^2 \right\}, \\
&\dots (14)
\end{aligned}$$

$$W_{r\Pi} = \int_0^\lambda ds \int_0^\infty V_\Pi dV_\Pi \int_0^{2\theta} \int_{v_r - \Delta v}^{v_r + \Delta v} dV_\Pi \frac{m_\alpha}{2} \left\{ (N + n_1)(V_\Pi + u_\Pi)^2 - NV_\Pi^2 \right\} \quad \dots (15)$$

For the resonant particles $\delta = 1$ and the resonant velocity V_r defined as

$$V_r = \frac{\omega - l\Omega_i}{k_\Pi},$$

$$W_{r\perp} = \left(\frac{\lambda E^2}{8\pi} \right) \left(\frac{\omega^2}{\Omega_\alpha^2} \right) \left(\frac{\omega}{k_\Pi V_{th\alpha}} \right) \frac{\Omega_\alpha t}{\sqrt{2\pi}} \exp \left\{ -\frac{1}{2} \left(\frac{\omega}{k_\Pi V_{th\alpha}} \right)^2 \left(1 - \frac{\lambda\Omega_\alpha}{\omega} \right)^2 \right\} \quad \dots (16)$$

$$\times \frac{1}{2} \langle J_{\lambda-1}^2 + J_{\lambda+1}^2 \rangle \left[1 - \left(\frac{R \left(\frac{\lambda\Omega_\alpha}{\omega} - 1 \right)}{\frac{\lambda\Omega_\alpha}{\omega}} \right) \frac{T_{\perp\alpha}}{T_{\Pi\alpha}} \right]$$

$$W_{r\Pi} = \left(\frac{\lambda E^2}{8\pi} \right) \left(\frac{\omega^2}{\Omega_\alpha^2} \right) \left(\frac{\omega}{k_\Pi V_{th\alpha}} \right) \frac{\Omega_\alpha t}{\sqrt{2\pi}} \exp \left\{ -\frac{1}{2} \left(\frac{\omega}{k_\Pi V_{th\alpha}} \right)^2 \left(1 - \frac{\lambda\Omega_\alpha}{\omega} \right)^2 \right\} \quad \dots (17)$$

$$\times \frac{1}{2} \langle (J_{\lambda-1} + J_{\lambda+1})^2 \rangle \left[\frac{\left(1 - \frac{\lambda\Omega_\alpha}{\omega} \right)}{\frac{\lambda\Omega_\alpha}{\omega}} \right] \frac{T_{\perp\alpha}}{T_{\Pi\alpha}}$$

$$\text{Where, } R = \frac{(J_{l+1} + J_{l-1})^2}{\langle J_{l+1}^2 + J_{l-1}^2 \rangle}$$

$$\langle J_l^2(\mu) \rangle \approx \langle (J_{l+1}(\mu) + J_{l-1}(\mu))^2 \rangle \left(\frac{\mu^2}{4l^2} \right)$$

Using the law of conservation of energy the growth rate is obtained to be

$$\left| \frac{dW_{r\perp}^\alpha}{dt} \right| \left| \frac{dW_{r\Pi}^\alpha}{dt} \right|$$

Hence the growth rate is,

$$\frac{\gamma}{\omega} = \sqrt{\frac{\pi}{2}} \left(\frac{\omega}{k_\Pi V_{th\alpha}} \right) \left(1 - \frac{\lambda\Omega_\alpha}{\omega} \right)^2 \exp \left\{ -\frac{1}{2} \left(\frac{\omega}{k_\Pi V_{th\alpha}} \right)^2 \left(1 - \frac{\lambda\Omega_\alpha}{\omega} \right)^2 \right\} \quad \dots (18)$$

$$\times \left[R \left(\frac{\lambda\Omega_\alpha}{\omega} - 1 \right) \frac{T_{\perp\alpha}}{T_{\Pi\alpha}} - 1 \right]$$

For $J = 0$ the growth rate reduces to that given by Terashima³³.

3 Results and Discussion

We have evaluated the dispersion relation, transverse energies and growth/damping rate of EIC waves in multi-component plasma. A graphical representation of the expressions is shown in Figs 1-12. The following parameters relevant to the auroral acceleration region are used^{9,20} to evaluate the dispersion relation, resonant energies and growth rate.

$$B_0 = 4300nT \text{ at } 1.4 R_E; \Omega_H^+ = 412 \text{ s}^{-1}; \Omega_{He^+} = 206 \text{ s}^{-1}; \Omega_0^+ = 51.50 \text{ s}^{-1}; \lambda = 300m;$$

$$E_l = 50mV/m; k_{ll} = 2m^{-1}; \frac{T_{ll\alpha}}{T_{\perp\alpha}} = 5eV; d_{lle} = 52.55m$$

Using these data in derived expression for dispersion relation (Eq. 12), perpendicular resonant energy (Eq. 16), parallel resonant energy (Eq. 17) and growth rate (Eq. 18) we obtain the graphical representations.

Figures 1-3 show the variation of wave frequency ω (s^{-1}) verses perpendicular wave number $k_\perp \rho_i$ for multi-ions (H^+ , He^+ , O^+) with $J=0, 1$ and 2 . It is found that the loss-cone distribution enhanced the wave frequency of multi-ions due to loss-cone structure of magnetosphere. More energetic particles are available to provide energy to the wave by wave particle interaction. For lighter (H^+ , He^+) ions it attains a peak and shifts towards right due to shifting in the resonance condition while for heavier ion (O^+) after attaining a peak wave frequency becomes constant it may be due to its heavier mass.

The H^+ ions are in cyclotron resonance with the wave and participate more effectively in energy exchange process as compared to He^+ & O^+ ions. Ahirwar *et al.*⁹ have stated that the FAST (Fast Auroral Snapshot) satellite has detected a class of ions

conics events in which H_e^+ ions is more strongly accelerated than H^+ or O^+ ions. The transverse acceleration of ion is a usual and normal process in the high latitude auroral ionosphere that is approximately coincident with the auroral oval. The steep loss-cone affects the heating rate of the transversely accelerated ions through the EIC instability in the auroral acceleration region. The auroral acceleration region

accelerates both ions upward along magnetic field lines, while electrons downwards which creates the visible aurora. The ions precipitates in the energy exchange process are predominant due to direct injection into the loss-cone in this region.

Figures 4-6 represents the variation of growth rate γ / ω versus perpendicular wave number $k_{\perp} \rho_i$ with

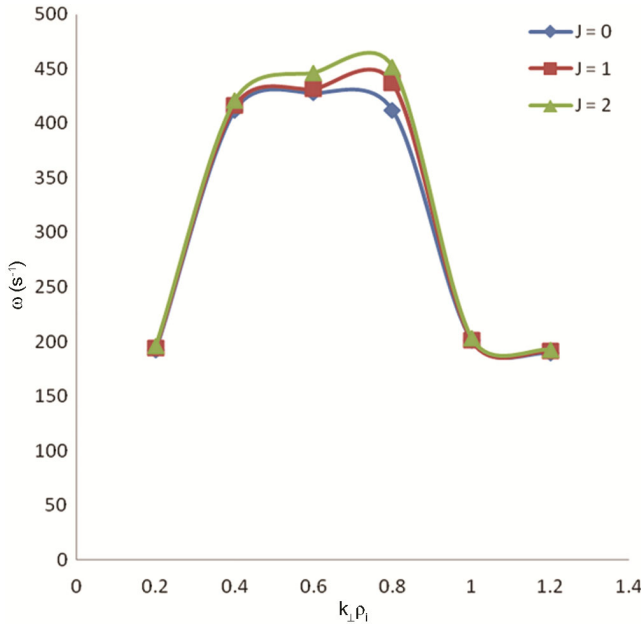


Fig. 1 — Variation of wave frequency ω (s⁻¹) versus $k_{\perp} \rho_i$ for hydrogen ion at $J=0, 1$ and 2

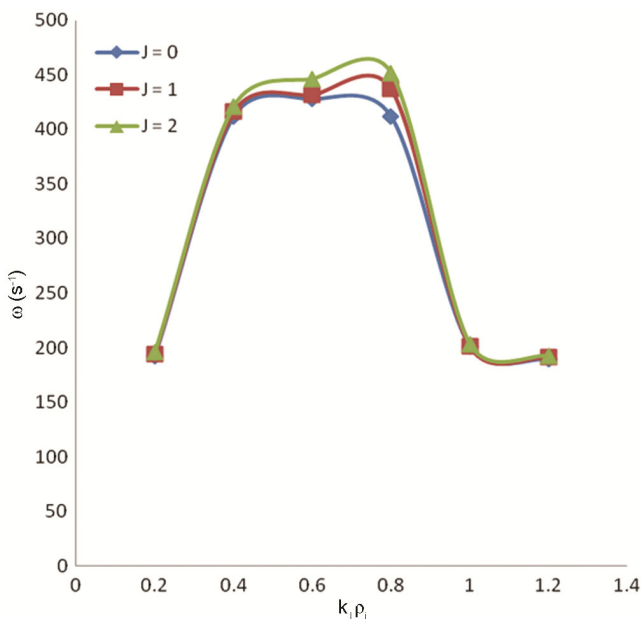


Fig. 2 — Variation of wave frequency ω (s⁻¹) versus $k_{\perp} \rho_i$ for helium ion at $J=0, 1$ and 2

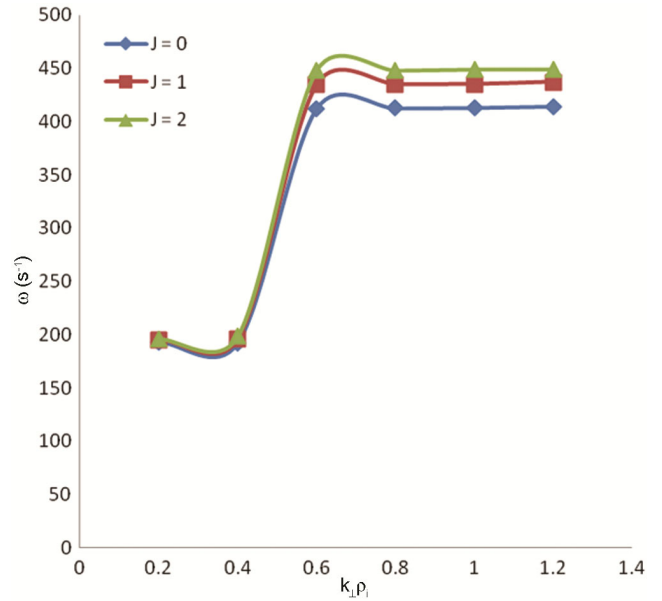


Fig. 3 — Variation of wave frequency ω (s⁻¹) versus $k_{\perp} \rho_i$ for oxygen ion at $J=0, 1$ and 2

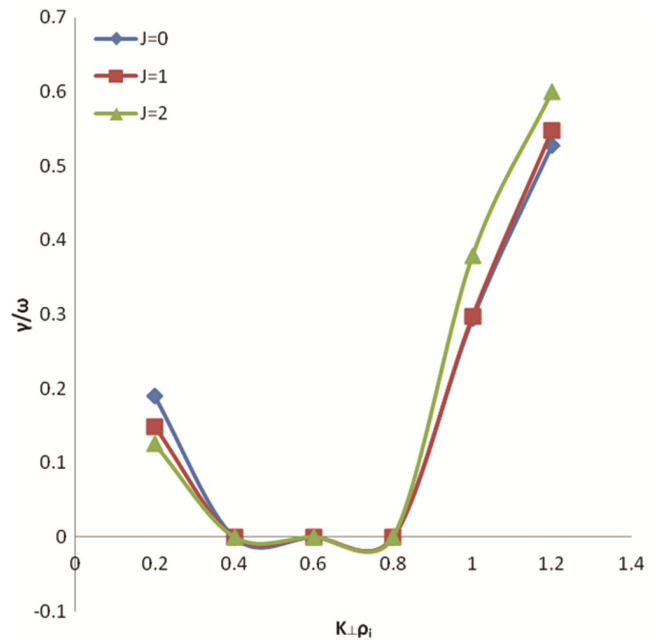


Fig. 4 — Variation of growth rate γ / ω versus $k_{\perp} \rho_i$ for hydrogen ion at $J=0, 1$ and 2

multi-ions (H^+ , He^+ , O^+) for different values of distribution index $J=0,1$ & 2. It is found that steepness of loss-cone enhances the growth rate of the wave for multi-ions, it is due to particle impart energy to the wave by wave particle interaction. For H^+ ion the growth rate with perpendicular wave number first decreases then increases. For He^+ and O^+ ions growth rate decrease with perpendicular wave number, i. e., the wave impart energy to the particles of heavy mass. For He^+ ion growth rate attains a peak and shifts towards right due to shifting in the resonance condition.

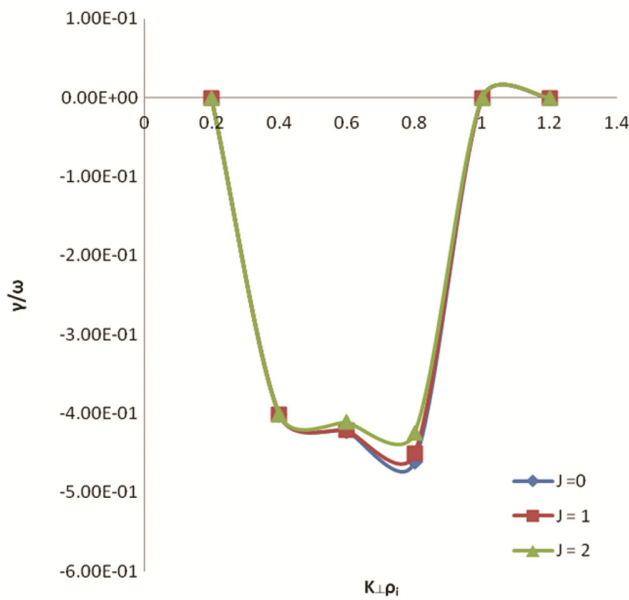


Fig. 5 — Variation of growth rate γ/ω versus $k_{\perp}\rho_i$ for helium ion at $J=0, 1$ & 2

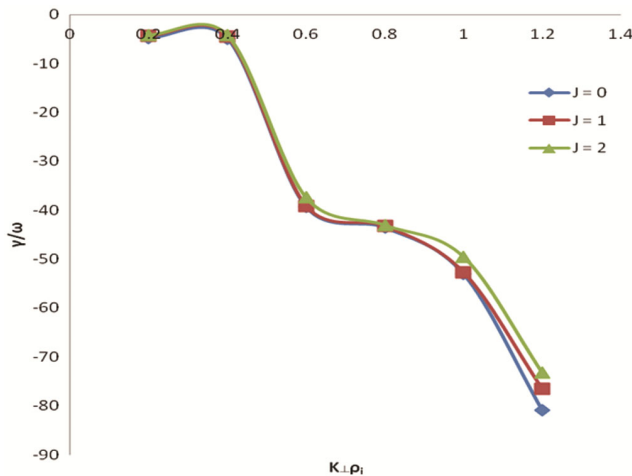


Fig. 6 — Variation of growth rate γ/ω versus $k_{\perp}\rho_i$ for oxygen ion at $J=0, 1$ and 2

The collision less wave particle scattering by EIC fluctuations is a possible explanation for these results. The steep loss-cone structures are analogous to mirror like devices with higher mirror ratio that may accelerate the charged particles moving perpendicular to the magnetic field. Therefore, the more energetic particles may be available to provide energy to the EIC wave by resonance wave-particle interactions.

Figures 7-9 show the variation of perpendicular resonant wave energy $w_{r\perp}$ (erg/cm) versus perpendicular wave number $k_{\perp}\rho_i$ with multi-ions (H^+ , He^+ , O^+) for

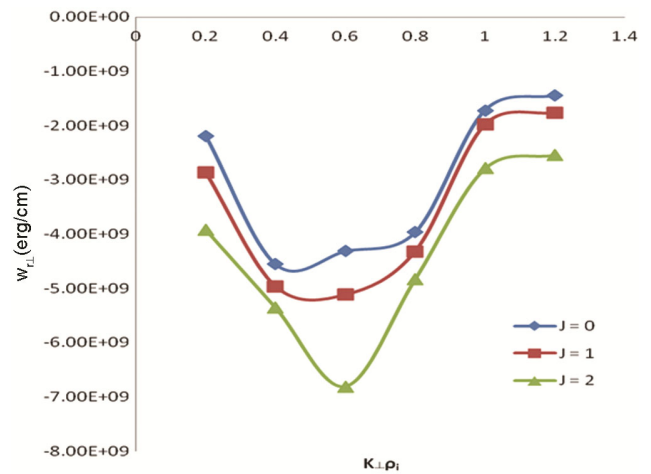


Fig. 7 — Variation of perpendicular resonant energy $w_{r\perp}$ (erg/cm) versus $k_{\perp}\rho_i$ for hydrogen ion at $J=0, 1$ and 2

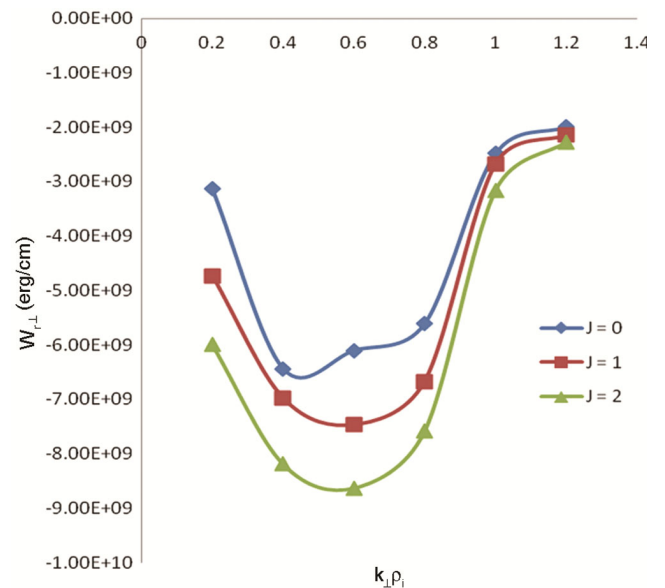


Fig. 8 — Variation of perpendicular resonant energy $w_{r\perp}$ (erg/cm) versus $k_{\perp}\rho_i$ for helium ion at $J=0, 1$ and 2

different values of distribution function $J=0,1$ & 2. It is observed that perpendicular resonance energy is decreased due to the steepness of the loss-cone distribution for lighter ions (H, He). For the lighter ions (H^+ , He^+) perpendicular resonance energy of the wave is decreased and attains a peak at 0.6 and resonance condition shifting toward higher wave

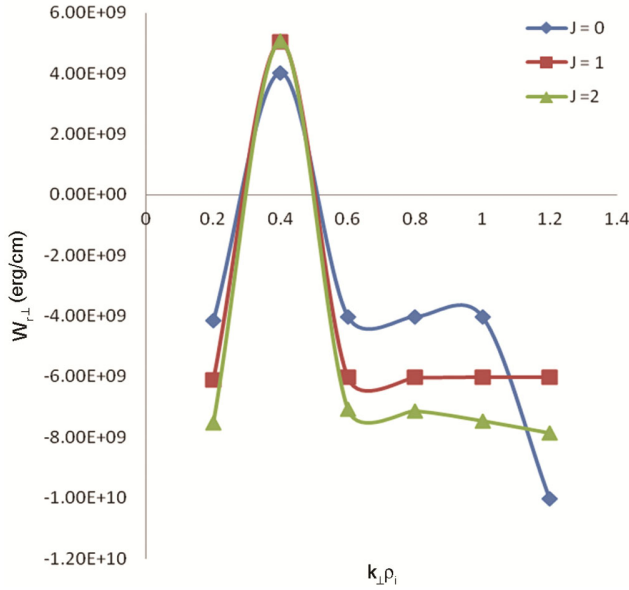


Fig. 9 — Variation of perpendicular resonant energy $w_{r\perp}$ (erg/cm) versus $k_{\perp}\rho_i$ for oxygen ion at $J=0, 1$ and 2

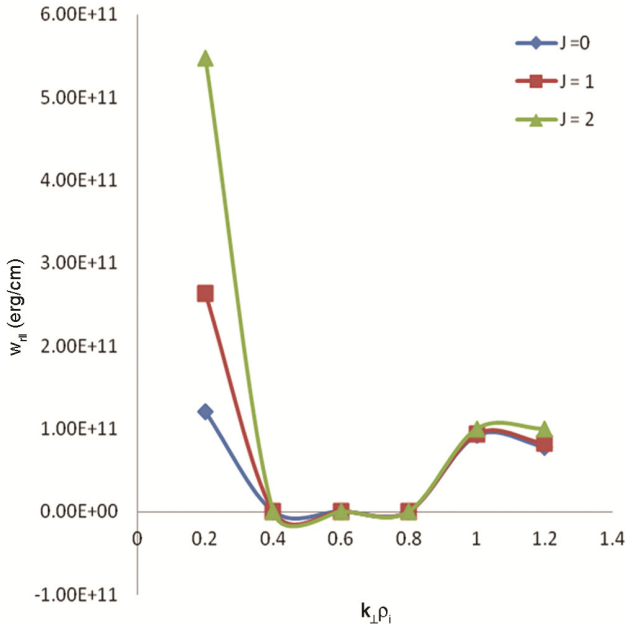


Fig. 10 — Variation of parallel resonant energy $w_{r\parallel}$ (erg/cm) versus $k_{\perp}\rho_i$ for hydrogen ion at $J=0, 1$ and 2

numbers according to distribution index due to the impart of the energy to the wave by particle. For heavier ions (O^+) the energy is increased according the increase of distribution index. For heavier ions (O^+) by increasing the perpendicular wave number perpendicular resonant energy attains a peak at 0.4. It is due to the resonance condition of the wave particle interaction.

The steep loss-cone distribution of the magnetosphere decreases the transverse energy as the wave frequency approaches the cyclotron frequency. The positive energy represents the transfer of energy from the wave to resonant ions whereas the negative energy represents the transfer of energy from the resonant ions to the wave. It is observed that the particular values of the distribution index J the transfer of the energy from the wave to the resonant ions decreases with perpendicular wave number and after that the energy is transferred from the resonant ions to the wave.

Figures 10-12 show the variation of parallel resonant energy versus perpendicular wave number with $J=0, 1$ & 2 . It is observed that the distribution index stabilize the parallel resonant energy it may be due to mirror like structure of magnetosphere, i. e., trapped energetic particles provide energy to the wave. With perpendicular wave number parallel resonant energy first decreases then increases for H^+ ions and for He^+ ions it decreases with perpendicular wave number. For O^+ ions it stabilized with perpendicular wave number and attains a peak which shifts towards right due to shifting in the resonance condition.

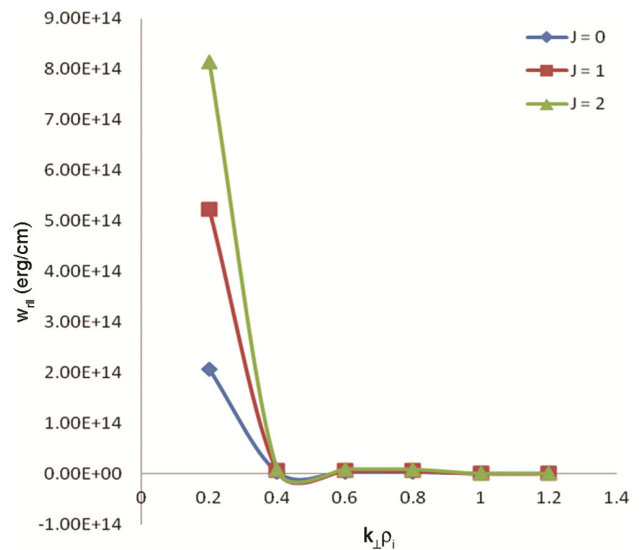


Fig. 11 — Variation of parallel resonant energy $w_{r\parallel}$ (erg/cm) versus $k_{\perp}\rho_i$ for helium ion at $J=0, 1$ and 2

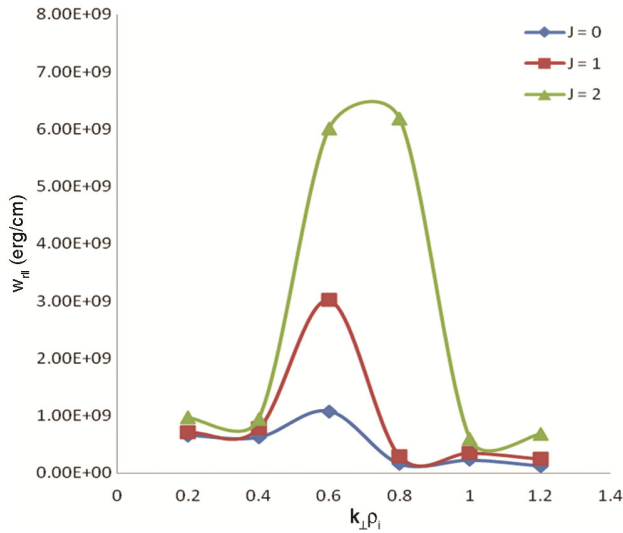


Fig. 12 — Variation of parallel resonant energy $w_{||}$ (erg/cm) versus $k_{\perp} \rho_i$ for oxygen ion at $J = 0, 1$ and 2

The effect of general loss-cone distribution function with distribution index on EIC waves with multi-ions magnetospheric plasma has been studied. It is found that the steepness of loss-cone distribution function decrease perpendicular resonant heating of O^+ ion, while enhances parallel resonant heating it due to wave particle resonance. It also decreases the growth rate of wave. Barghouthi *et al.*³⁴ shown that the behavior of O^+ ion total actual heat flux in auroral acceleration region is similar to its behavior in the polar wind, except that the magnitudes are higher in the auroral region and tend to increase at a slow rate at altitude above $5R_E$ in the polar wind region and at altitudes above $2R_E$ in the auroral region.

In the auroral region the magnitudes of H^+ and O^+ ion total heat fluxes are on the same order. That is the same amount of energy transferred from low altitude to higher by both ions is similar. For H^+ ion actual total heat flux is negative at very low altitudes (i.e., around $1.8R_E$). This means that energy is going downward along the geomagnetic field lines. Barghouthi *et al.*³⁴ stated that parallel and perpendicular heat fluxes have different signs above results shows correlation with our results in auroral acceleration region. By comparing with “thermalized” heat flux, Barghouthi *et al.*³⁴ found that O^+ and H^+ ion outflow in the auroral region in the altitude range $1.2-3R_E$. This is equivalent to our prediction of auroral acceleration region, i.e., $1.4R_E$. The size of mirror structure was about one-gyro radii. Axelsson *et al.*³⁵ used optical data from the Auroral Large Imaging System (ALIS) to perform a statistical

study of spatial and temporal variation of diffuse auroral structures.

Ge *et al.*³⁶ reported the mirror model structure these structures were observed by the THEMIS-D spacecraft this has analogy with our loss-cone distribution function. Magnetic mirroring makes possible the “trapping” in the dipole-like field lines near Earth of particles in the radiation belts, in the inverted “V” structures of auroral acceleration region and in the ring current. Such lines the field is much stronger at their ends near Earth, compared to its strength when it crosses the equatorial plane. Assuming such particles are somehow placed in the equatorial region of that field, most of them stay trapped, because every time their motion along the field line brings them into the strong field region, they “get mirrored” and bounce back and forth between hemispheres. Only particles, whose motion is close to parallel to the field line, with near-zero magnetic moment, avoid mirroring and these are quickly absorbed by the atmosphere and lost. Their loss leaves a bundle of directions around the field line which is empty of particles the “loss cone”.

Based on our prediction distribution index ‘ J ’ is a measure of steepness of loss-cone feature. It characterizes the width of loss-cone, if steepness will be enhanced then more and particles that are more energetic will be available to provide energy to the wave in auroral acceleration region. In presence of loss-cone distribution, the transfer of energy from the parallel component of the plasma ions to the EIC through the wave particle interaction takes place. Distribution index J is slightly increases the parallel resonant energy at lower perpendicular perturbations but at higher perpendicular perturbation, the distribution index J enhanced the transfer of energy from the parallel component of the resonant ions to the EIC waves. The O^+ ions are more effective as compare to H^+ and He^+ ions^{9,37}. The steep loss-cone distribution enhances the wave’s emissions of the EIC waves as well as the heating of the multi-ions parallel to the magnetic field by extracting the energy of the perpendicularly heated ions. The mirroring force may become operative in association with EIC waves in order to control the heating and to emit the wave.

4 Conclusions

In this paper we have conducted a comprehensive mathematical analysis of EIC waves with multi-ions plasma (H^+ , He^+ and O^+) and found how the wave is grown through the inverse landau damping as well as

the wave particle interactions. The effect of the general loss-cone distribution function is incorporated in the auroral acceleration region to discuss these waves emissions with multi-ions plasma. The steep loss-cone structure are analogous to mirror-like devices with a higher mirror ratio, which accelerate the charged particles perpendicular to the magnetic field and that may be a free energy source to excite EIC waves. Thus, particles that are more energetic may be available to provide energy to the wave by wave-particles interactions. The converging magnetic field lines in the higher latitude auroral ionosphere may be considered suitable for the use of generalized loss-cone distribution function.

The altitude around $1.4R_E$ is supposed as auroral acceleration region where waves can impart energy to the particles. The process can be conveyed to the outer magnetosphere at higher altitudes as well as towards the lower ionosphere by wave-particle interaction mechanism. Theory may be useful to interpret the electrodynamics of the auroral ionospheric region. The EIC turbulence may play an important role in the loss-cone current-potential relationship. The steep loss-cone distribution, enhance the growth rate and anomalous resistivity may play a crucial role in the auroral acceleration region. The particle aspect analysis developed may be applicable to laboratory and space plasmas, as well as to estimate the heating and acceleration of charged particles along with the study of emissions of EIC waves. The plasma waves can transfer energy from ring current H^+ to O^+ during magnetic storms^{38,39} and play an important role in the heating of the thermal electrons and ions⁴⁰. The present analysis may be useful to explain heating of He^+ , O^+ ions, this heating of heavier ions is known as differential heating.

It was observed from the observations by FAST satellite that the ion cyclotron waves in association with the ion-conics may play a significant role in transverse acceleration of ions in auroral acceleration region⁴¹. It is reasonable to assume that if ion cyclotron waves are present in the solar corona, then the heavy ions will strongly affect the ion cyclotron wave spectrum. In future present study can be extended for storms times, which is generated by solar phenomena like solar flares and coronal mass ejections. These studies may help to predict the disruptions of communication during the storm times. Using this mathematical model and extending

for various conditions can be used to predict the shape of the magnetosphere.

Acknowledgment

The authors (PV) and (BDR) thankfully acknowledge to DST and UGC, respectively, for financial assistance.

References

- 1 Klumpar D M, *J Geophys Res*, 84 (1979) 4229.
- 2 Frank L A, Ackerson K L & Yeager D M, *J Geophys Res*, 82 (1977) 129.
- 3 Ono M, Porkolab M & Chang R P H, *J Phys Fluids*, 23 (1980) 1656.
- 4 Abraham N P, Sreekala G, Sebastian S, Michal M, Mathew P, Aamir M, Jayapal R, Renuka G & Venugopal C, *Int J Sci Res*, 3 (2014) 1290.
- 5 Zhao K, Jiang Y, Ding L & Huang L, *Planet Space Sci*, 101 (2014) 170.
- 6 Simic D & Gajic D, *Phys Chem Technol*, 5 (2007) 45.
- 7 Kurian M J, Jyothi S, Leju S K, Issak M, Venugopal C & Renuka G, *J Phys*, 73 (2009) 1111.
- 8 Rosenberg M & Merlino R L, *J Plasma Phys*, 1 (2008) doi: 10.1017/8002237808007642.
- 9 Ahirwar G, Varma P & Tiwari M S, *Indian J Pure Appl Phys*, 48 (2010) 334.
- 10 Temrin M & Roth I, *Astrophys J*, L105 (1992) 391.
- 11 Hamrin M, Norquist P, Hellstorm T, Andre M & Eriksson A I, *Ann Geophys*, 20 (2002) 1998.
- 12 Summers D & Throne R M, *J Geophys Res*, 108(A4) (2003) 1143. doi: 10.1029/2002JA009489.
- 13 Albert J M, *J Geophys Res*, 108(A6) (2003) 1249 doi:10.1029/2002JA009792.
- 14 Engebretson M J, Lessard M R & Bortnik J, *J Geophys Res*, 113 (2008) A01211, doi:10.1029/2007JA012362.
- 15 Kim Su-Hyun, Agrimson E, Miller M J, D'Angelo N & Merlino R L, *Phys Plasmas*, 11 (2004) doi: 10.1063/1.1780531.
- 16 Strelstov A V, *J Geophys Res*, 116 A10203 (2011) doi:10.1029/2011JA016550.
- 17 Pandey R S & Kaur R, *Adv Space Res*, 56 (2015) 714-724.
- 18 Kindel J M & Kennel C F, *J Geophys Res*, 76 (1971) 3055.
- 19 Drummond W E & Rosenbluth M N, *J Phys Fluids*, 5 (1962) 1507.
- 20 Mishra R & Tiwari M S, *Planet Space Sci*, 54 (2006) pp 188.
- 21 Kennel C F & Petschek H E, *J Geophys Res*, 71 (1966) 1-28 DOI: 10.1029/JZ071i001p00001.
- 22 Temerin M & Lysak R L, *J Geophys Res*, 89 (1984) doi: 10.1029/JA089iA05p02849 ISSN: 0148-0227.
- 23 Cattell C A, Mozer F S, Roth I, Anderson R R, Elphic R C, Lennartsson W & Ungstrup E, *J Geophys Res*, 96 (1991) doi:10.1029/91JA00378. ISSN: 0148-0227.
- 24 McFadden J P, Ergun R E & Elphic R, *Geophys Res Lett*, 25 (1998a) 2045-2048.
- 25 Erlandson R E & Zanetti L J, *J Geophys Res*, 103 (1998) 4627-4636.
- 26 Chaston C C, Ergun R E & Delory G T, *Geophys Res Lett*, 25 (1998) 2057-2064.
- 27 Mishra R & Tiwari M S, *Indian J Pure Appl Phys*, 43 (2005) 377.
- 28 Mishra R & Tiwari M S, *Earth Moon Planets*, 100 (2007) 195.

- 29 Tiwari M S & Varma P, *Planet Space Sci*, 41 (1993) 199.
- 30 Hirose A, *Phys Fluids*, 19 (1976) 272-275.
- 31 Summers D & Throne R M, *J Plasma Phys*, 53(3) (1995) 293-315.
- 32 Mishra K D & Tiwari M S, *Can J Phys*, 57 (1979) 1124.
- 33 Terashima Y, *Prog Theor Phys (Japan)*, 37 (1967) 661.
- 34 Barghouthi I A, Nilsson H & Ghithan S H, *Ann Geophys*, 32 (2014) 1043.
- 35 Axelsson K, Sergienko T, Nilsson H, Brandstrom U, Ebihara Y, Asamura K & Hirahara M, *Ann Geophys*, 30 (2012) 1693.
- 36 Ge Y S, McFadden J P, Raeder J, Angelopoulos V, Larson D & Constantinescu O D, *J Geophys Res*, 116 (2011) A01209, doi:10.1029/2010JA015546.
- 37 Raikwar B D, Varma P & Tiwari M S, *Astrn Space Sci*, 2 (2016) 1-10.
- 38 Thorne R M & Horne R B, *J Geophys Res*, 99 (1994) 17 275-17 282.
- 39 Thorne R M & Horne R B, *J Geophys Res*, 102 (1997) 14155-14163.
- 40 Horne R B & Thorne R M, *J Geophys Res*, 102 (1997) 11 457-11 471.
- 41 Lund E J, Mobius E, Carlson C W, Ergun R E, Kistler L M, Klecker B, Klumpar D M, McFadden J P, Popecki M A, Strangeway R J & Tung Y K, *J Atmos Sol-Terr Phys*, 62 (2000) 467-475.